

UC Irvine

UC Irvine Previously Published Works

Title

Effect of Faraday rotation on L-band interferometric and polarimetric synthetic-aperture radar data

Permalink

<https://escholarship.org/uc/item/2st7d2gh>

Journal

IEEE Transactions on Geoscience and Remote Sensing, 38(1)

ISSN

0196-2892

Author

Rignot, EJM

Publication Date

2000

DOI

10.1109/36.823934

Copyright Information

This work is made available under the terms of a Creative Commons Attribution License, available at <https://creativecommons.org/licenses/by/4.0/>

Peer reviewed

Effect of Faraday Rotation on L-Band Interferometric and Polarimetric Synthetic-Aperture Radar Data

Eric J. M. Rignot

Abstract—Electromagnetic waves traveling through the ionosphere undergo a Faraday rotation of the polarization vector, which modifies the polarization and phase characteristics of the electromagnetic signal. Using L-band ($\lambda = 24$ cm), polarimetric synthetic aperture radar (SAR) data from the shuttle imaging radar C (SIR-C) acquired in 1994, we simulate the effect of a change in the Faraday rotation angle ψ on spaceborne interferometric and polarimetric data. In one experiment, we find that phase coherence is reduced by up to 33% when ψ changes between successive data acquisitions. If ψ changes by more than 40° , a differential phase signal, which varies from field to field, appears in the interferogram and impairs the mapping of surface topography and/or the detection of ground deformation. This signal is caused by phase differences between horizontal-polarized and vertical-polarized radar signals from intermediate levels of vegetation canopy, similar to the phase difference measured between H-polarized and V-polarized signals on a single date. In a second experiment, data from the Japanese Earth Resources Satellite (JERS-1) L-band radar acquired in an area of active deforestation in Rondonia, Brazil, are compared with SIR-C L-band polarimetric data acquired at the same incidence, two weeks later, but from a lower orbiting altitude. Large differences in scattering behavior are recorded between the two datasets in the areas of slash and burn forest, which are difficult to reconcile with surface changes. A simulation with SIR-C polarimetric data, however, suggests that those differences are consistent with a Faraday rotation angle of about $30 \pm 10^\circ$ in the JERS-1 data and 0° in the SIR-C data. Based on these two experiments and on global positioning system (GPS) records of ionospheric activity, we conclude that Faraday rotation should not affect the analysis of L-band spaceborne data during periods of low ionospheric activity (solar minima). Yet during ionospheric storms or near solar maxima, the effects should become significant and impair data analysis. Corrections for Faraday rotation are impractical in the case of single-channel SAR data. SAR data must be acquired with the full polarimetry to recover from these effects.

Index Terms—Ionosphere, SAR interferometry, SAR polarimetry.

I. INTRODUCTION

ELECTROMAGNETIC waves traveling through the ionosphere interact with the electrons and the magnetic field with the result that the polarization vector of the electric field is rotated by an angle ψ called the Faraday rotation angle [10, ch. 8, p. 272]. Other effects of the ionosphere include propagation delays of the radar echoes, ray bending, radiowave scintillation, and phase changes. While these effects are all of importance

for the processing of multichannel and interferometric synthetic aperture radar (SAR) data, we focus the present discussion on the effect of changes in the Faraday rotation angle on the polarimetric and interferometric characteristics of SAR data acquired from a spaceborne platform.

If one assumes an ionosphere with a vertically and horizontally constant electron-density profile and a constant field direction along the entire path [10, p. 275], the Faraday rotation angle ψ may be expressed as

$$\psi = 2.610^{-13} \text{TEC } B \lambda^2 \cos(\theta) \quad (1)$$

where

- ψ is in radians and TEC in electrons/meter² is the total electron content of the slab of ionosphere below which the radar measurements are collected;
- B Earth's magnetic field in Tesla;
- λ radar wavelength in meters;
- θ angle between the magnetic field and the radar illumination in radians.

Equation (1) illustrates that ψ scales with the square of the radar wavelength, so it is 16 times larger at L-band (24-cm wavelength) than at C-band (5.6-cm wavelength). In addition, the TEC can vary by one order of magnitude between day and night as solar illumination exerts a dominant control on ionospheric density. The Faraday rotation angle also varies with latitude and is larger at the tropics than at the poles for the same radar-illumination angle.

The peak ionospheric density occurs at about 400 km altitude (Fig. 1). Low-orbiting (200-km altitude) radar systems of the class of the Shuttle Imaging Radar C (SIR-C) are not expected to be affected by the ionosphere. A SAR of the class of the Japanese Earth Resources Satellite (JERS-1), an L-band SAR orbiting at 575 km altitude, however, sends and receives radar signals through most of the ionosphere. The effect should be negligible at C-band frequency (at this frequency, a typical value of ψ is a few degrees during the day, which is about the noise level of the phase measurements, and fractions of a degree at night), but not at L-band or lower radar frequencies.

Radar astronomers who operate long-wavelength, ground-based radars to probe planetary objects solved the problem by operating those radars at circular polarization [3]. Faraday rotation is not a factor at circular polarization. For monitoring applications of the Earth's surface, however, operating a radar at circular polarization may not be optimal for retrieval of geophysical parameters such as vegetation biomass or soil moisture, because these techniques typically require the full scattering matrix for each resolution element. Moreover, most inversion techniques being developed today are based on

Manuscript received January 30, 1998; revised May 5, 1999. This work was supported by the National Aeronautics and Space Administration, Washington, DC.

The author is with the Jet Propulsion Laboratory, California Institute of Technology, Pasadena, CA 91109-8099 USA (e-mail: eric@adelle.jpl.nasa.gov).

Publisher Item Identifier S 0196-2892(00)00409-5.

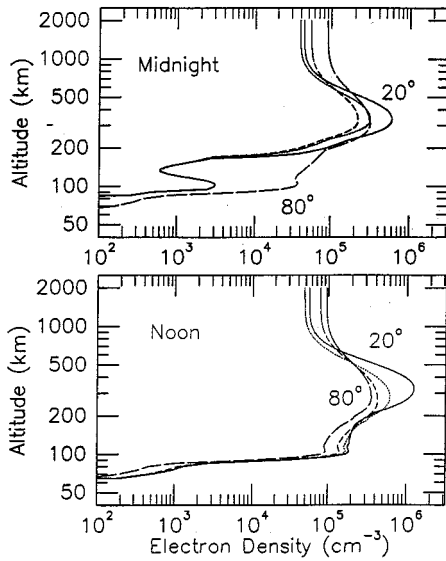


Fig. 1. International Reference Ionosphere (1985) calculation of the electron-density height profile for a variety of latitudes and at midnight and noon (P. Rosen, personal communication, 1997). Longitude is 293° east and latitudes are 20° (solid line), 40° (dotted), 60° (dashed), and 80° (long dashed) north. SIR-C orbited at about 200 km altitude. JERS-1 orbited at about 575 km altitude.

data acquired by spaceborne/airborne SAR's operating at linear polarization.

In the case of a linear-polarized radar system [e.g., JERS-1's L-band HH-polarized (horizontal transmit and receive) system], the effect of Faraday rotation is to rotate the polarization vector of the electric field clockwise by an angle ψ during transmission of the signal down through the ionosphere. Upgoing from the surface, the polarization vector of the electric field will undergo another Faraday rotation in the same sense relative to the Earth's magnetic field. As a result, the scattering properties of the surface will appear different to the radar compared to the case where Faraday rotation does not affect the signal (e.g., on an airborne platform). Furthermore, if the Faraday rotation angle ψ varies from one passage of the satellite to the next, the quality and information content of repeat-pass SAR interferometric and of changes in radar backscatter will be modified.

In this study, we use SAR data from low-orbitting and high-orbitting satellites to evaluate how Faraday rotation could impact practical interferometry and polarimetry applications at the L-band frequency. We estimate the effect of changes in ionospheric density on phase coherence and on data interpretability. We compare SAR data acquired by SIR-C and JERS-1 at the same site, incidence, time of year, but acquired from different orbiting altitudes. Based on the results, we draw conclusions concerning the possible effect of changes in ionospheric density on data from current or future orbiting spaceborne L-band SAR's.

II. METHODS

The SIR-C instrument records the complete scattering matrix \mathbf{S} of each resolution cell by combining transmit and receive signals at horizontal (H) and vertical (V) linear polarization

$$\mathbf{S} = [S_{HH}, S_{HV}, S_{VH}, S_{VV}] \quad (2)$$

where the S_{XY} 's are the complex scattering amplitudes at X -polarization transmit and Y -polarization receive. If p_r and p_t are, respectively, the polarization vector of the receive and transmit antennas, the complex amplitude of the receive signal may be expressed as

$$V = p_r^t \mathbf{S} p_t. \quad (3)$$

If the signal is affected by Faraday rotation, the scattering matrix \mathbf{S} will be modified by Faraday rotation once downgoing and another time upgoing from the radar to become

$$\mathbf{M} = \mathbf{F} \mathbf{S} \mathbf{F} \quad (4)$$

where the Faraday rotation matrix \mathbf{F} is

$$\mathbf{F} = [\cos(\psi), \sin(\psi), -\sin(\psi), \cos(\psi)]. \quad (5)$$

The modified scattering matrix \mathbf{M} is

$$\begin{aligned} M = & [S_{HH} \cos^2(\psi) - S_{VV} \sin^2(\psi), \\ & S_{HV} + (S_{HH} S_{VV}) \sin(\psi) \cos(\psi), \\ & S_{HV} - (S_{HH} S_{VV}) \sin(\psi) \cos(\psi), \\ & S_{VV} \cos^2(\psi) - S_{HH} \sin^2(\psi)] \end{aligned} \quad (6)$$

where we assumed that $S_{HV} = S_{VH}$ from the reciprocity principle. Equation (6) shows that a radar system operating at HH polarization above the ionosphere will in effect measure radar returns that are a mixture of H-polarized and V-polarized returns. Moreover, there will be a significant amount of crosstalk between the H-channel and V-channel, since M_{HV} is not equal to M_{VH} .

For the purpose of our simulation study, we assume that ψ does not vary spatially within one scene (100 km) in (6) and that other effects of the ionosphere (e.g., time delays, scintillation, etc.) are negligible. To simulate the response of a natural target in the presence of Faraday rotation, we calculate the new scattering-matrix angle \mathbf{M} using (6) and substitute it for \mathbf{S} in (3). Concerning the reference date, we use HH-polarization (i.e., $\psi = 0$) as the reference polarization state. On the second date, we assume a Faraday rotation angle ψ between 0° (horizontal polarization) and 90° (vertical polarization).

The discussion focuses on two aspects of Faraday rotation. The first aspect is how Faraday rotation affects the temporal coherence and physical nature of the interferometric phase recorded from repeat-pass data. A second aspect is how data interpretation in terms of surface processes is affected by Faraday rotation. For the first aspect, we use SIR-C data acquired in the Mahantango Creek Watershed, PA, for which both polarimetric and interferometric L-band data were available. For the second aspect, we compare SIR-C polarimetric L-band data acquired in Rondonia, Brazil, with JERS-1 SAR data.

III. STUDY SITES

The Mahantango Creek Watershed SIR-C hydrology test site is located at 76.6° W, 40.7° N, in eastern Pennsylvania, near the city of Sunbury. It is an area of adjacent valleys and ridges resulting from the formation of the Appalachian mountains several hundred million years ago. Ridge tops are forest-covered. Valleys comprise cleared land and farm fields. The $11 \text{ km} \times 50 \text{ km}$ scene shown in Fig. 2(a) was acquired at 46° incidence angle

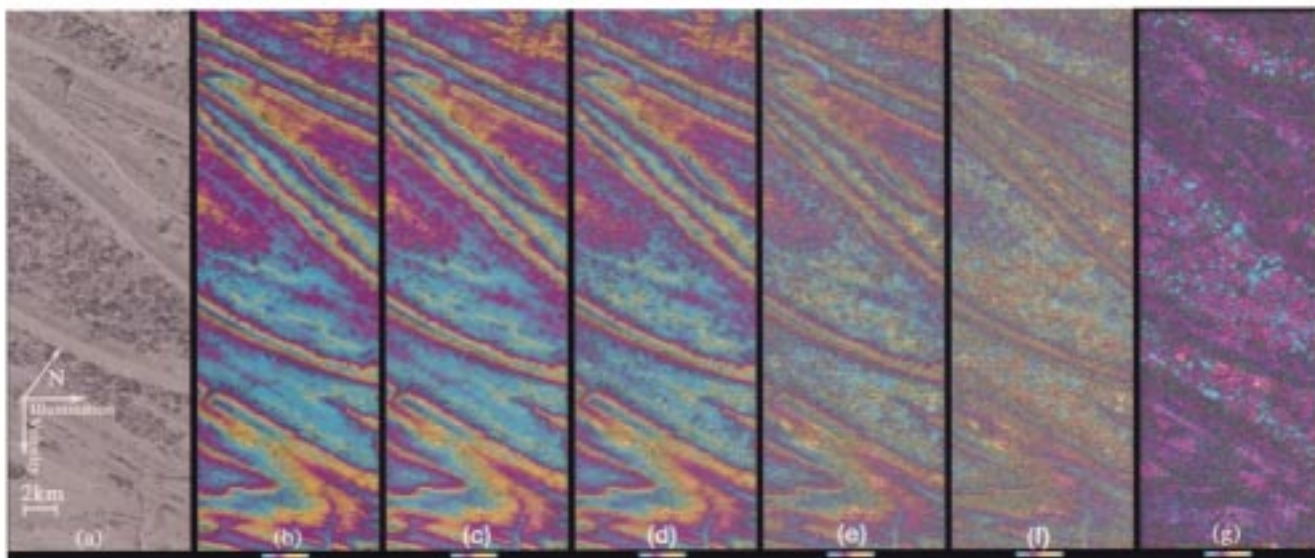


Fig. 2. SIR-C image of the Mahantango Creek Watershed, PA, located at 76.6° west, 40.7° north. The scene is $11 \text{ km} \times 50 \text{ km}$ in size, acquired at 46° incidence angle, during orbit 150 of SIR-C, on Oct. 9, 1994, at 10:08 am local time: (a) amplitude image at L-band HH-polarization and (b) radar interferogram combining L-band HH-polarized data acquired on Oct. 9 and 10, 1994. Each fringe or full-color cycle represents a 360° variation in phase, here equivalent to a 450-m change in surface height. Interferograms combining L-band HH from Oct. 9 with no Faraday rotation and L-band HH from Oct. 10 with a Faraday rotation angle ψ equal to (c) 30° , (d) 45° , (e) 60° , and (f) 90° (hence, equivalent to L-band VV-polarization from Oct. 10). The color intensity of each interferogram is modulated by phase coherence (see text). Areas of low phase coherence have a darker tone. Phase coherence is decreasing from (b)–(f), and (g) differential interferogram combining L-band HH acquired on Oct. 9 and L-band VV acquired on Oct. 10 after removal of an interferometric topographic map obtained using L-band HH on Oct. 9 and L-band HH on Oct. 10.

during orbit 150 of SIR-C, on Oct. 9, 1994, at 10:08 am local time, with both L- and C-band fully polarimetric.

The second site is located 50 km southeast of the city of Porto Velho, in Rondonia, Brazil, in an area of active deforestation that we studied previously using SIR-C, JERS, Landsat, and Satellite Pour l'Observation de la Terre (SPOT) data [8]. The region is traversed by highway BR-364 built in 1984. Much of the land is in pasture of various quality for cattle, and secondary growth of various ages. SIR-C data were collected over that site at 02:18 am local time, during orbit 94 of SIR-C, at a center location of $8^\circ 58'$ south, $63^\circ 17'$ west on Oct. 6, 1994, at an incidence angle of 37° at the image center, with C-band and L-band fully polarimetric. The same area was imaged on Sept. 22, 1994 and Oct. 23, 1995 by the JERS SAR, which operates at 35° incidence, L-band HH-polarization. Sept.–Oct. corresponds to the peak of the dry season in Rondonia and is the time of year when most land clearance occurs. JERS and SIR-C data were acquired at the same frequency, same incidence, but from different orbiting altitudes.

IV. INTERFEROMETRIC RESULTS

A radar interferogram of the Mahantango Creek Watershed generated at L-band HH-polarization is shown in Fig. 2(b), using data collected one day apart. The component of the interferometric baseline perpendicular to the line of sight of the radar B_\perp is 60 m. The altitude of ambiguity of the phase data is 450 m, meaning that each interferometric fringe in the interferogram represents a 450-m change in surface elevation. Comparing this interferometric map with a topographic map of the area produced by the U.S.G.S., we estimated the root mean square (RMS) error of the interferometrically-derived height

map to be about 15 m. The interferometric map obtained at C-band (not shown here) yields a phase-coherence level that is too low to convert the interferometric data into a height map.

Fig. 2(c)–(f) shows the interferometric fringes corresponding to different values of the Faraday rotation angle ψ for the second data acquisition. When $\psi > 30^\circ$, the phase noise increases at a detectable level over most of the scene. The reduction in fringe visibility is more apparent in Fig. 2(e) and (f) as ψ becomes larger. The phase-coherence reduction is largest for $\psi = 90^\circ$. More important, the fringe pattern changes when ψ is large. The effect is most noticeable for $\psi > 60^\circ$. For instance, look in the oval-shaped valley area in the center of the scene.

To illustrate the observed change in phase signal, we removed the height map derived from the L-band HH-polarization data from the interferogram shown in Fig. 2(f). The result, shown in Fig. 2(g), is a differential phase signal, about one third of a cycle in amplitude, which homogeneously varies from field to field. Fields exhibiting little or no differential-phase signal tend to correspond to bare surfaces, whereas fields exhibiting large phase differences correspond to crops. Forested areas developing on the valley ridges behave differently depending on whether they are facing the radar illumination or not.

The decrease in phase coherence associated with the change in the Faraday rotation angle is plotted in Fig. 3. Phase coherence is here calculated as

$$\rho = \left| \frac{\langle \mathbf{a}_1 \mathbf{a}_2^* \rangle}{\langle |\mathbf{a}_1|^2 \rangle \langle |\mathbf{a}_2|^2 \rangle} \right| \quad (7)$$

where \mathbf{a}_1 and \mathbf{a}_2 are, respectively, the complex amplitude measured by the SIR-C antenna at time t_1 (reference date, with no Faraday rotation) and time t_2 (second date, with Faraday rotation). The operator $\langle \rangle$ means spatial average, and the operator

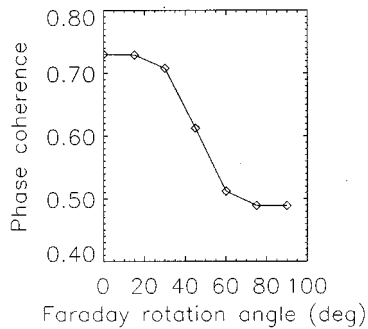


Fig. 3. Decrease in phase coherence of the radar interferogram shown when the Faraday rotation angle ψ in Fig. 2 increases from (a) 0° to (g) 90° .

$\|$ takes the modulus of a complex number. Here, spatial averaging used eight samples (the interferogram had eight looks), and we plotted the average phase coherence for the whole scene in Fig. 3.

Phase coherence is reduced by 16% when $\psi = 45^\circ$, but it is not zero when $\psi = 90^\circ$. This means that the scattering centers are not completely independent at the two polarizations. There is, however, a difference in scattering pathlength between H-polarized and V-polarized signals, because there exists a nonzero differential phase between the two polarizations. This phase differential resembles that measured between H-polarized and V-polarized signals on a single date, also known as the HH-VV polarimetric phase difference. If phase coherence was unity in the multirate data, the differential phase would indeed be equal to the HH-VV polarimetric phase difference. Phase coherence is not unity, however, because of temporal changes in the scattering characteristics of the surface, so the phase difference measured from the multirate data is noisier than that measured on a single date.

Phase coherence is reduced more significantly over forested areas (ridges and portions of the valley) than over crops (valleys). We attribute this behavior to lower correlation of the H-polarized and V-polarized signals over heavily vegetated terrain (such as forest), because of the dominance of volume-scattering interactions. Over bare surfaces, surface-scattering interactions dominate, H-polarized and V-polarized signals are more strongly correlated, and the differential interferogram between L-band HH and VV exhibits higher levels of phase coherence.

If the interferogram shown in Fig. 2(f) were used to generate a height map, height errors in excess of several hundred meters would result from the phase difference between H-polarized and V-polarized signals. Similarly, if the interferogram were used to measure ground deformation, it would detect a signal of about one third of a cycle, which does not correspond to an actual motion of the surface but to a difference in scattering pathlength between H-polarized and V-polarized signals, which is surface and incidence-angle dependent.

This difference in scattering pathlength is consistent with the expectation that H-polarized signals penetrate deeper into the vegetation canopy than V-polarized signals and with less attenuation. Indeed, we verified that the scattering centers at V-polarization in the SIR-C data were located above those at H-polarization, because the phase differential between day 2 (V-po-

larized) and day 1 (H-polarized) is always positive (the phase in Fig. 2 increases from blue to red, yellow and blue again, as the distance to the radar decreases).

V. SIR-C, JERS COMPARISON

Fig. 4 shows a SIR-C image acquired at L-band HH-polarization, a JERS-1 image acquired two weeks earlier at the same frequency and polarization and a JERS-1 image acquired one year later.

The two instruments operate at the same incidence angle and the same radar frequency and polarization. The bright patches of cleared forests appearing in the SIR-C images were identified in the field as associated with slash and burn areas, meaning areas where the forest had been cut and burned for the first time, leaving a complex chaos of burned and semi-burned trees, most of them lying flat on the ground, with only a few remaining standing trees [8]. These areas are typically abandoned for a year until they are burned again. The process is repeated several times until the land is transformed into pasture.

The radar backscatter of slash and burn areas in the SIR-C data is brighter than that of the surrounding forest at HH-polarization because of the preferred horizontal polarization of the scatterers (downed tree trunks). This phenomenon was first observed in SIR-B data of the Amazon [9]. In contrast, the same areas are darker than the surrounding forest in the 1994 and 1995 JERS images. In Oct. 1995, our field observations indicated that most slash and burn areas were still in some stage of clearing/reburning, with a large number of dead trunks covering the ground. Hence, the difference in scattering behavior between SIR-C and JERS cannot be attributed to the removal of tree trunks.

Fig. 5 shows a simulation of what an L-band HH image would look like for various Faraday rotation angles if the SIR-C data had been acquired at the same altitude as JERS's. Note how the bright radar signatures of slash and burn areas in (a) progressively disappear to be replaced by dark radar signatures at VV-polarization (e). Similarly, flooded areas marked in (a) change dramatically in radar backscatter. The dark radar signature at VV-polarization is consistent with the fact that most tree trunks lying on the ground act as discrete horizontal dielectric cylinders, hence producing strong scattering at H-polarization and weak scattering at V-polarization [11].

The simulation suggests that JERS-1 data (f) acquired a few weeks prior to the SIR-C flight resemble the SIR-C data with a Faraday rotation angle of $30 \pm 10^\circ$ (b) and (c). For instance, the areas of slash and burn marked at the bottom of (a) are darker in (d), but yet not as dark as in the JERS-1 data (f). The 1995 data [Fig. 4(c)] show less contrast between slash and burn areas and the surrounding forest than the 1994 data, which could be attributed to enhanced Faraday rotation or, more likely, to other effects such as vegetation regrowth (which would attenuate the returns from the horizontal dead trunks) or changes in soil and vegetation moisture.

The SIR-C data should not be sensitive to Faraday rotation, because the Shuttle orbited below most of the ionosphere. Indeed, a low level of cross-talk between H- and V-channels (-33 dB) was consistently measured during both SIR-C experiments

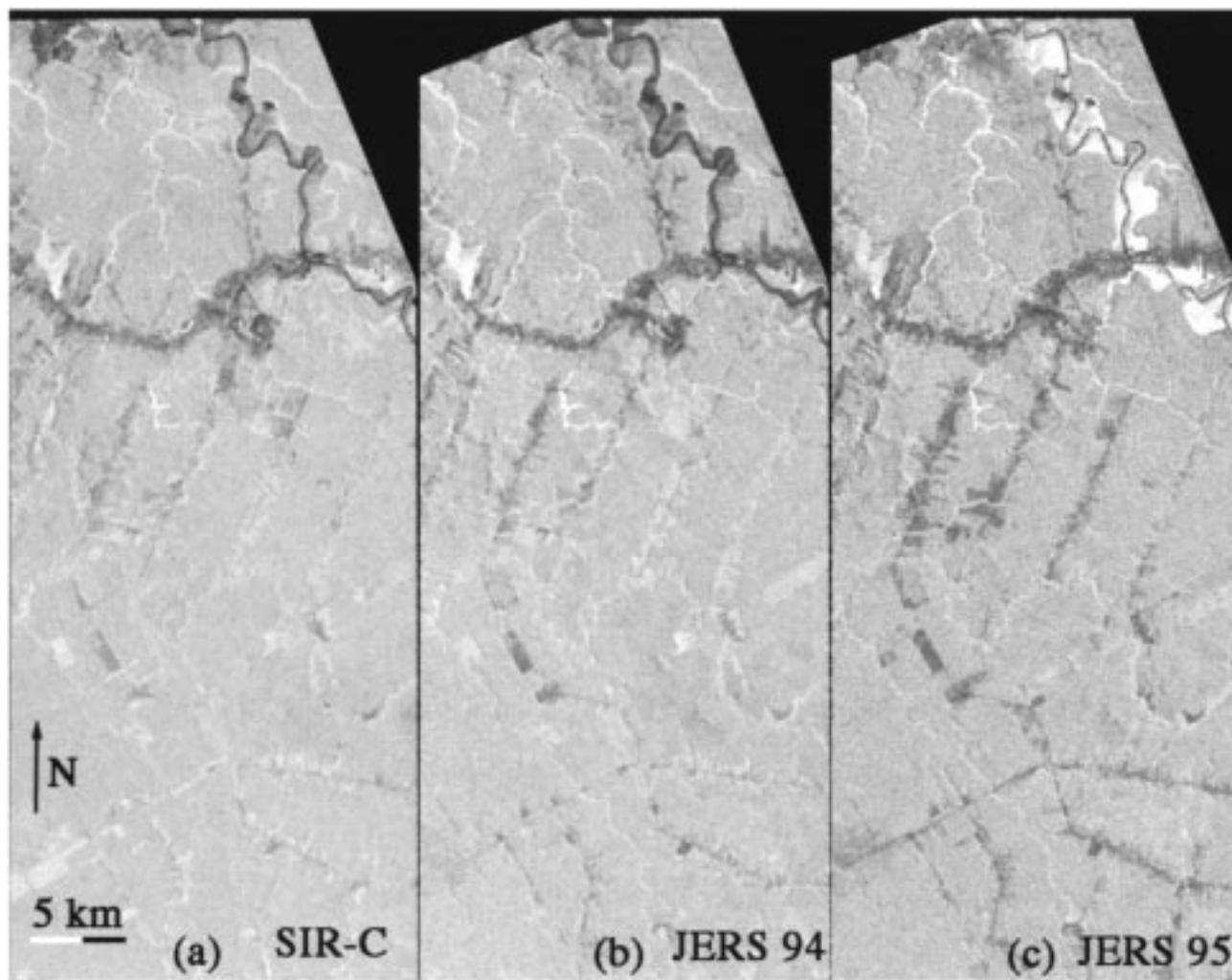


Fig. 4. Radar-amplitude image of a deforestation test site in the state of Rondonia, Brazil, located 50 km southeast of the city of Porto Velho, at $8^{\circ} 58' S$ and $63^{\circ} 17' W$: (a) L-band HH SIR-C image acquired on Oct. 7, 1994, and $20.7 \text{ km} \times 25 \text{ km}$ in size, (b) L-band HH JERS-1 image acquired on Sept. 22, 1994 (path/row is 418/316), and (c) L-band HH JERS-1 image acquired on Oct. 23, 1995.

day and night [4], which would not have been the case in the presence of Faraday rotation [see also (6), which shows that M_{HV} (second term of right-hand side of the equation) is not equal to M_{VH} (third term) when ψ is nonzero]. In contrast, data acquired at 575 km altitude at L-band frequency by JERS-1 should be affected by Faraday rotation (Fig. 1).

If JERS-1 SAR is indeed affected by a detectable level of Faraday rotation, it explains why the range of radar backscatter values recorded by JERS-1 SAR over tree stands of various biomass is only of 2–3 dB [7], compared to the 5–6 dB reported from airborne experiments at L-band HH-polarization [2]. Similarly, the increase in radar backscatter associated with forest regrowth in the Amazon and measured by JERS-1 SAR is less than that expected from those same airborne experiments [6] and is in fact closer to that expected from an L-band VV-polarized system. Faraday rotation also explains why slash and burn areas are typically darker in the JERS data than in the SIR-B and SIR-C data. In effect, the JERS-1 SAR system does not measure the true HH-polarized response of the terrain, but some mixture of its HH-polarized and VV-polarized responses. As known from airborne radar experiments, VV-polarization is less

sensitive to woody biomass than HH-polarization, so L-band HH-polarized data collected from above the ionosphere should indeed exhibit less sensitivity to woody biomass (and to horizontally-oriented objects such as slash and burn areas) than data collected from below the ionosphere.

VI. RELEVANCE OF THE SIMULATIONS

Fig. 6 illustrates how the level of ionospheric-integrated density or total electron content (TEC), measured by GPS, varies from year to year and increases with the level of solar activity [5]. The TEC changes by one order of magnitude from month to month or even on a daily basis within the same month. Since the Faraday rotation angle is directly proportional to the TEC [see (1)], it means that ψ can increase by one order of magnitude during periods of high ionospheric activity (solar maximum) compared to periods of low ionospheric activity (1990 was the last solar maximum and 2001 will be the next).

Using the IRI 1995 standard ionosphere model (http://nssdc.gsfc.nasa.gov/space/model/models/iri_n.html) we estimated the expected level of ionospheric activity at the

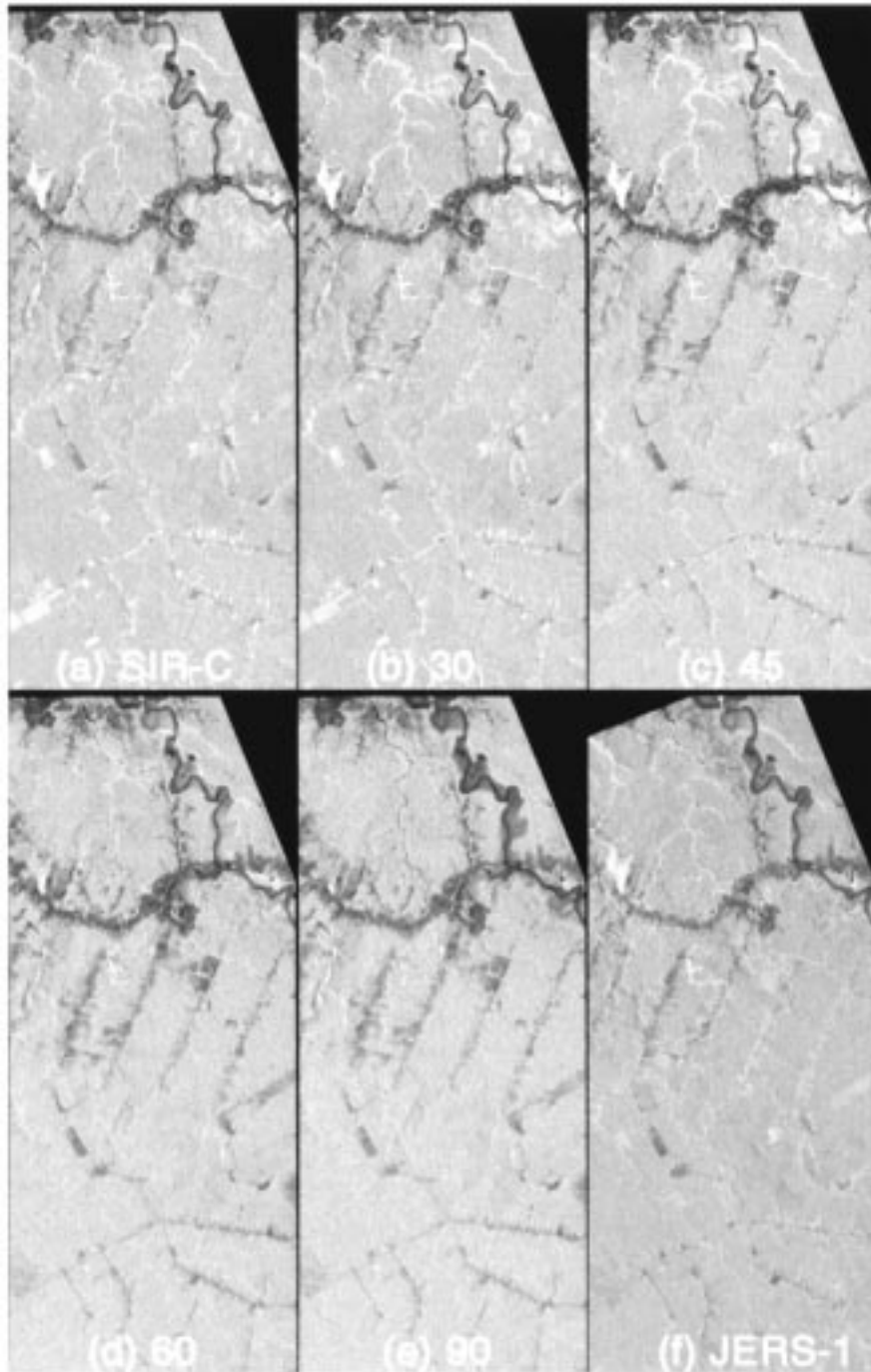


Fig. 5. Simulation of the effect of the Faraday rotation angle on SIR-C data of the Rondonia test site, Brazil. Radar amplitude image for (a) $\psi = 0^\circ$ (i.e., L-band HH-polarization), (b) 30° , (c) 45° , (d) 60° , and (e) 90° (i.e., L-band VV-polarization). Panel (f) shows the JERS-1 image acquired on Oct. 7, 1994. Areas of slash and burn [radar bright in (a)] become darker than the surrounding forest from (a)–(f), as ψ increases toward 90° .

location (-9° latitude, 297° longitude) and time (14 UTC) of passage of the JERS-1 satellite over Rondonia. Integrating the IRI 1995 predictions of electron content per meter³ along the path of the radar illumination (0–575 km), we find a nominal TEC of 3×10^{17} electrons/m² almost identical on both dates. Using $B = 0.5 \times 10^{-4}$ Tesla, $\lambda = 24$ cm, and $\theta = 60^\circ$ in (1), we deduce $\psi = 11^\circ$. This prediction from a standard ionosphere model is low, as it corresponds to a period of low solar activity (1995 was a solar minimum). It is also low compared to the results of the SIR-C/JERS simulation (which

suggests $30 \pm 10^\circ$), which may be due to limitations of the ionosphere model or to changes of another nature affecting the JERS-1 data (e.g., changes in soil and vegetation moisture in the two weeks prior to the SIR-C overflight).

Hence, outside periods of solar maxima and/or ionospheric storms, with a TEC varying anywhere between 10^{17} and 5×10^{17} electrons/m² at noon, changes in the Faraday rotation angle should not exceed 10° and therefore should not be a problem. During solar maxima or ionospheric storms, the results in Fig. 6 suggest that the TEC could increase by a factor

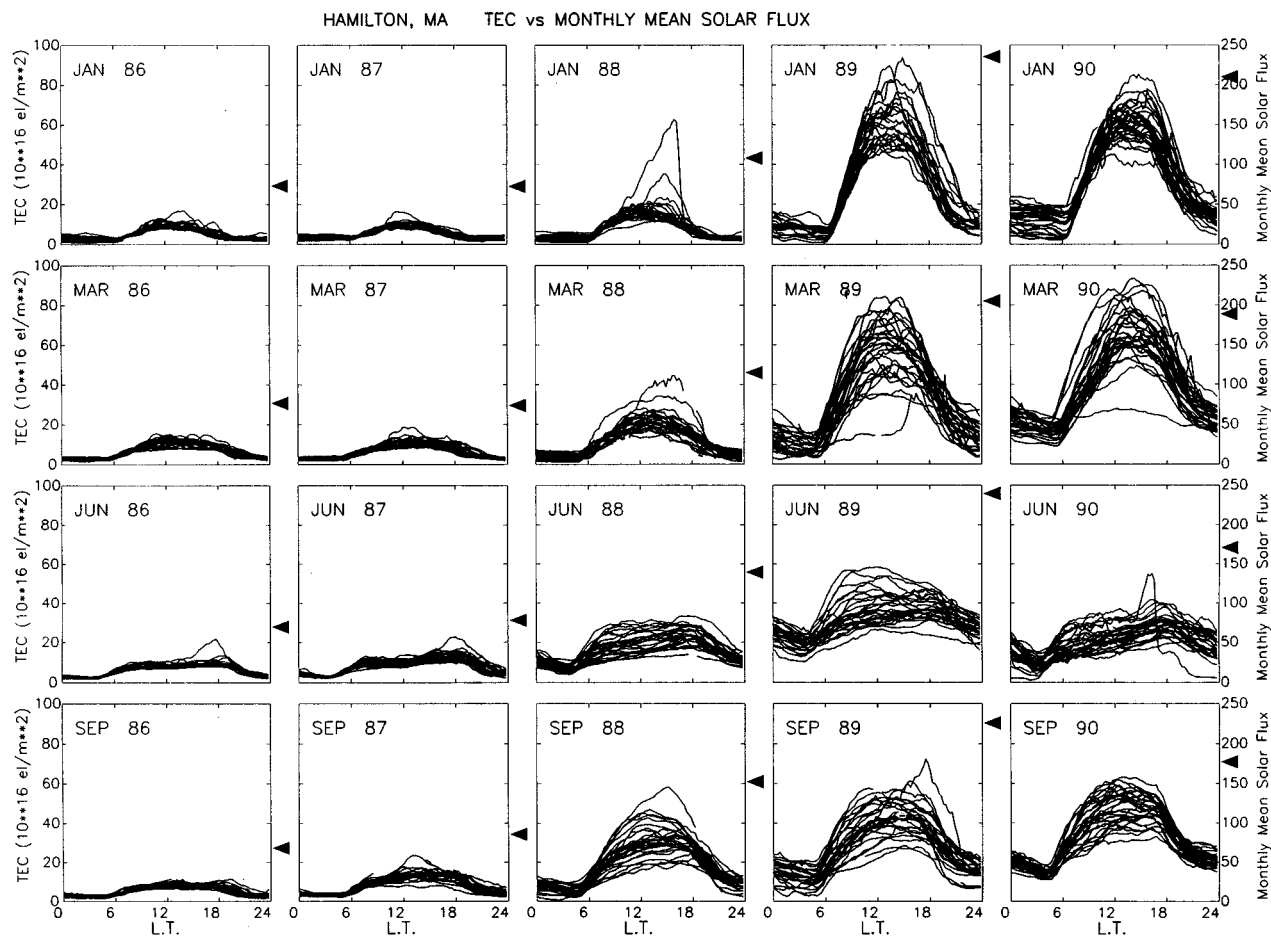


Fig. 6. Long-term plot of TEC from Hamilton, MA (38.7 N, 70.7 W) near vertical incidence. Each chart is a plot of diurnal TEC behavior for each day in the month indicated. Dependence on solar cycle is displayed from left to right (solar minimum in 1986 to maximum in 1990). Seasonal dependence for a given year is displayed from top to bottom. This plot was obtained courtesy of P. Doherty and J. Klobuchar (private communication, 1997).

ten, making it possible for ψ to even reach 90° , which would definitely create problems interpreting temporal changes in phase and radar backscatter.

VII. CONCLUSIONS

Using SAR data from the SIR-C and JERS-1 missions, we evaluated the effect of changes in ionospheric density on polarimetric and interferometric SAR data at the L-band frequency. We find that Faraday rotation of several tens of degrees significantly changes the radar amplitude and phase characteristics of remotely-sensed surfaces, and that the time variability of the phenomena may be a limiting factor for change detection and interferometry applications. Existing records of ionospheric-integrated density suggest that large variations in ionospheric density exist on a daily to yearly time scale. Near solar maxima or during ionospheric storms, high-orbiting spaceborne radar systems operating at L-band could be affected by Faraday rotation angles of several tens of degrees larger than usual.

To circumvent this limitation, one possibility is to design and operate the radar with circular polarization, as commonly

done in radar astronomy. Most research work conducted using earthborne SAR's however, is based on using linear polarization data. A second solution is to operate the radar at a higher radar frequency, for instance, S-band (10-cm wavelength) instead of L-band (24-cm wavelength), and thereby reduce the magnitude of the disturbances by a factor of ≈ 6 . Research experience with S-band data is limited however, except for data acquired by the Earth-orbiting Almaz SAR system and the Venus-orbiting Magellan Radar System. A third possibility is to estimate the amount of ionospheric-integrated density, for instance using GPS, and use those estimates to tag bad SAR data with unusual (high) levels of ionospheric degradation. Whatever the estimation technique, however, the "true" polarization state of the data will not be restituted, because that operation requires the full scattering matrix [1]. Similarly, the true phase of the signal will not be restituted to correct differential interferometry data. A fourth and probably better solution is to operate the radar with the full polarimetry. In this case, the Faraday rotation angle (and possibly other effects of the ionosphere) could, in principle, be estimated from the radar data directly, and the true polarization state and phase of the signal could be properly restituted, calibrated, and interpreted.

ACKNOWLEDGMENT

The author thanks J. van Zyl and P. Rosen for stimulating discussions about this topic, and T. Mannucci, P. Doherty, and J. Klobuchar for helpful discussions and for providing the TEC plot in advance of publication. We also thank the reviewers of the manuscript for their precious and helpful comments.

REFERENCES

- [1] K. Davies, *Ionospheric Radio Propagation*. Washington, DC: United States Dept. Commerce, 1965, pp. 210–214.
- [2] M. C. Dobson, F. T. Ulaby, T. LeToan, A. Beaudoin, E. S. Kasischke, and N. Christensen, "Dependence of radar backscatter on conifer forest biomass," *IEEE Trans. Geosci. Remote Sensing*, vol. 30, pp. 412–415, Mar. 1992.
- [3] J. V. Evans, "Radar astronomy," *Contemporary Phys.*, vol. 2, p. 116, 1960.
- [4] A. Freeman *et al.*, "SIR-C data quality and calibration results," *IEEE Trans. Geosci. Remote Sensing*, vol. 33, pp. 848–857, July 1995.
- [5] J. A. Klobuchar and P. H. Doherty, "Expected ionospheric effects on GPS signals in the year 2000," *GPS Solutions*, 1997, submitted for publication.
- [6] A. Luckman, J. Baker, T. M. Kuplich, C. D. F. Yanasse, and A. C. Frery, "A study of the relationship between radar backscatter and regenerating tropical forest biomass for spaceborne SAR instruments," *Remote Sens. Environ.*, vol. 60, no. 1, pp. 1–13, 1997.
- [7] Ministry of International Trade and Industry, "Final report of JERS-1/ERS-1 system verification program," NASDA, Tokyo, Japan, vol. 2, Mar. 1995.
- [8] E. Rignot, W. Salas, and D. Skole, "Mapping deforestation and secondary growth in Rondonia, Brazil using imaging radar and thematic mapper data," *Remote Sens. Environ.*, vol. 59, pp. 167–179, July 1997.
- [9] T. A. Stone and G. M. Woodwell, "Shuttle imaging radar A analysis of land use in Amazonia," *Int. J. Remote Sensing*, vol. 9, pp. 95–105, Jan. 1988.
- [10] A. R. Thompson, J. M. Moran, and G. W. Swenson, *Interferometry and Synthesis in Radio Astronomy*. New York: Wiley, 1986.
- [11] J. J. van Zyl, "The effect of topography on radar scattering from vegetated areas," *IEEE Trans. Geosci. Remote Sensing*, vol. 31, pp. 153–160, Jan. 1993.

Eric J. M. Rignot was born in Chambon sur Lignon, France. He received the Engineer's degree from the Ecole Centrale des Arts et Manufactures Paris, France, in 1985, the M.S. degree in astronomy from the University of Paris VI, France, in 1986, the M.S. degree in aerospace engineering and electrical engineering in 1987 and 1988, respectively, and the Ph.D. degree in electrical engineering in 1991 from the University of Southern California, Los Angeles.

He is currently a Research Scientist with the Radar Science and Engineering Section, Jet Propulsion Laboratory, Pasadena, CA. He is a Principal Investigator on several NASA-funded projects to study the mass balance of the Greenland and Antarctic ice sheets using radar interferometry combined with other methods, the interactions of ice shelves with ocean waters, and the dynamic retreat of Patagonian glaciers. His research interests are in geoscience applications of radar interferometry and polarimetry. He is also a Member of the NASA Earth Science Information Partners' Tropical Forest Information Center and of the Shuttle Radar Topography Mission (SRTM) Science Team.

Dr. Rignot received the JPL Lew Allen Director's Award for Excellence in 1998. He is a member of the American Geophysical Union and the International Glaciological Society.